SUPPLEMENTARY APPENDIX

Immune cell constitution in the tumor microenvironment predicts the outcome in diffuse large B-cell lymphoma

Matias Autio,[1,2,3*] Suvi-Katri Leivonen,[1,2,3*] Oscar Brück,[3,4,5] Satu Mustjoki,[3,4,5] Judit Mészáros Jørgensen,[6] Marja-Liisa Karjalainen-Lindsberg,[7] Klaus Beiske,[8] Harald Holte,[9] Teijo Pellinen[10] and Sirpa Leppä[1,2,3]

[1]Applied Tumor Genomics Research Program, Faculty of Medicine, University of Helsinki, Helsinki, Finland; [2]Department of Oncology, Helsinki University Hospital Comprehensive Cancer Center, Helsinki, Finland; [3]iCAN Digital Precision Cancer Medicine Flagship, Helsinki, Finland; [4]Translational Immunology Research Program and Department of Clinical Chemistry and Hematology, University of Helsinki, Helsinki, Finland; [5]Hematology Research Unit Helsinki, Helsinki University Hospital Comprehensive Cancer Center, Helsinki, Finland; [6]Department of Hematology, Aarhus University Hospital, Aarhus, Denmark; [7]Department of Pathology, Helsinki University Hospital, Helsinki, Finland; [8]Department of Pathology, Oslo University Hospital, Oslo, Norway; [9]Department of Oncology, and KG Jebsen Centre for B Cell Malignancies, Oslo University Hospital, Oslo, Norway and [10]Institute for Molecular Medicine Finland (FIMM), Helsinki, Finland

**MA and S-KL contributed equally as co-first authors.*

 doi:10.3324/haematol.2019.243626

Received: November 22, 2019.

Accepted: February 17, 2020.

Pre-published: February 20, 2020.

Correspondence: *SIRPA LEPPÄ* - sirpa.leppa@helsinki.fi

Immune cell constitution in the tumor microenvironment predicts the outcome in diffuse large B-cell lymphoma

Matias Autio[1,2*], Suvi-Katri Leivonen[1,2*], Oscar Brück[3,4], Satu Mustjoki[3,4], Judit Mészáros Jørgensen[5], Marja-Liisa Karjalainen-Lindsberg[6], Klaus Beiske[7], Harald Holte[8], Teijo Pellinen[9], and Sirpa Leppä[1,2]

[1]Applied Tumor Genomics Research Program, Faculty of Medicine, University of Helsinki, Helsinki, Finland;

[2]Department of Oncology, Helsinki University Hospital Comprehensive Cancer Center, Helsinki, Finland;

[3]Translational Immunology Research program and Department of Clinical Chemistry and Hematology, University of Helsinki, Helsinki, Finland;

[4]Hematology Research Unit Helsinki, Helsinki University Hospital Comprehensive Cancer Center, Helsinki, Finland

[5]Department of Hematology, Aarhus University Hospital, Aarhus, Denmark;

[6]Department of Pathology, Helsinki University Hospital, Helsinki, Finland;

[7]Department of Pathology, Oslo University Hospital, Oslo, Norway;

[8]Department of Oncology, and KG Jebsen Centre for B cell malignancies, Oslo University Hospital, Oslo, Norway

[9]Institute for Molecular Medicine Finland (FIMM), Helsinki, Finland

[*]Equal contribution

Supplementary Methods

Nanostring gene expression analysis

Total RNAs were isolated with RecoverAll™ Total Nucleic Acid Isolation Kit for FFPE (Life Technologies, Thermo Fisher Inc., Waltham, MA). Two or three 20 µM sections were cut from the FFPE blocks and processed according to the manufacturer's protocol. A total of 100 ng of RNA was hybridized overnight at 65°C with the Human PanCancer Immunoprofiling Panel codesets (XT-CSO-HIP1-12, NanoString Technologies, Seattle, WA). Purification and binding of the hybridized probes to the cartridge were performed on the nCounter Prep Station, followed by scanning the cartridge on the nCounter Digital Analyzer (Nanostring Technologies). The data were analyzed with nSolver 3.0 software (NanoString Technologies). The quality of the data was confirmed by using the default QC

settings, and normalization done using the geNorm algorithm[1]. The data were log2 transformed for subsequent analyses. Correlation matrix and heatmap were done with the JExpress 2012 software[2] using Pearson correlation with average linkage.

Multiplex IHC

Panels

	Panel 1	Panel 2	Panel 3	Panel 4
TSA-488 fitc	R-anti-Granzyme B (Abcam;ab4059) 1:500	R-anti-Lag3 (Abcam;180187, clone EPR4392(2)) 1:400	M-anti-CD4 (Thermo;MA5-12259, clone 4B12) 1:50	M-anti-Tbet (Abcam;91109, clone 4B10) 1:50
TSA-555 Cy3	M-anti-OX-40 (Thermo;14-1347-82, clone ACT35) 1:50	M-anti-PD-1 (LSBio;B12784, clone 3C6) 1:100	R-anti-CD3 (Thermo; MA5-14482, clone EP449E) 1:1500	R-anti-CD3 (Thermo; MA5-14482, clone EP449E) 1:1500
Alexa-647 Cy5	R-anti-Ki67 (Thermo;9106-S0, clone SP6) 1:200	R-anti-Tim3 (CST;45208, clone D5D5R) 1:100	R-anti-Tim3 (CST;45208, clone D5D5R) 1:100	M-anti-FoxP3 (Abcam;20034, clone 236A/E7) 1:25
Alexa-750 Cy7	M-anti-CD8 (Dako; M7103, clone C8/144B) 1:200	M-anti-CD8 (Dako; M7103, clone C8/144B) 1:200	M-anti-Lag3 (LSbio;C18692, clone 17B4) 1:50	R-anti-CD4 (Abcam;ab133616, clone EPR6855) 1:25
TSA-750 Cy7			R-anti-CD4 (Abcam; Ab133616, clone EPR6855) 1:1000	

Multiplex immunohistochemistry (mIHC) was performed as described in Blom et al 2017, with some modifications [3]. Briefly, the fluorescence signals from AlexaFluor488 and AlexaFluor555 channels were amplified using tyramide signal amplification (TSA) (PerkinElmer, Waltham, MA). A pair of primary antibodies raised in different species was used to detect additional two targets using AlexaFluor647 and AlexaFluor750 fluorochrome-conjugated secondary antibodies without amplification. Nuclei were counterstained using DAPI and slides were mounted and coverslips applied. In panel 3, due to a weak CD4 signal, CD4 was re-stained and TSA-amplified using TSA Biotin System (#NEL700A001KT, PerkinElmer) and Streptavidin, Alexa Fluor™ 750 conjugate (S21384, Thermo Fischer Scientific).

Imaging

Digital, fluorescence images of mIHC slides were acquired at 0.32 µm/pixel resolution using Metafer 5 system including Axio Imager.Z2 microscope (Zeiss, Germany) equipped with EC Plan-Neofluar 20x objective (NA 0.8), Metafer scanning platform with CoolCube 2 CCD camera (MetaSystems, Germany), PhotoFluor LM-75 metal halide light source (89 North, Williston VT), and DAPI, FITC, CY3, CY5, and CY7 filter sets. After image acquisition, images were converted to 8-bit JPEG2000 format (95% quality).

Image analysis

All image analyses were performed as done in using CellProfiler (version 2.2.0). Cell classes were determined using pixel co-localization analysis. Each channel intensity was thresholded using Adaptive Otsu. Double or triple channel positive pixels were determined with “MaskImage”. Then, thresholded channel pixel areas were determined with “MeasureImageAreaOccupied” and areal proportions were counted by dividing the area with pixel area occupied by all the channels combined (ImageMath Add command). Cell class areas were exported as CSV files with “ExportToSpreadsheet”. The quality of TMA cores was determined by visual inspection. TMA cores

with low quality (e.g. ruptured or folded tissue or staining artefact) were excluded from further analyses.

HLA-DR, HLA-ABC and β_2 microglobulin IHC analyses

To evaluate the expression of HLA-DR, HLA-ABC and β_2 microglobulin (B2M), IHC was performed on the TMAs with samples from 188 DLBCL patients using antibodies for HLA-DR (Abcam; ab80658, clone LN3), HLA-ABC (Abcam; ab70328, clone EMR8-5) and B2M (Dako; A0072), as previously described [4]. Based on the membranous staining, HLA-DR and HLA-ABC expression was scored as either negative, moderate or positive, and B2M expression was scored as either negative, perinuclear, moderate or positive as previously described [5]. Scoring was performed independently by MA and SKL. Of the HLA-DR, HLA-ABC, and B2M stainings 36, 37, and 39 samples, respectively, were excluded due to poor quality.

***In silico* immunophenotyping**

CIBERSORTx[6] (http://cibersortx.stanford.edu) was used on publicly available datasets[7-10] to infer the proportions and GEPs of infiltrating immune cells. CIBERSORTx is a deconvolution algorithm that allows users to process gene expression data representing a bulk admixture of different cell types, along with a signature matrix file that enumerates the genes defining the expression profile for each cell type of interest. CIBERSORTx derives a *p*-value for the deconvolution for each sample using Monte Carlo sampling, providing a measure of confidence in the results. As a signature file, we used a 547-gene Leukocyte gene signature matrix (LM22). Gene expression

datasets were uploaded to the CIBERSORTx web portal and the algorithm run using the LM22 signature matrix at 100 permutations.

References

1. Vandesompele J, De Preter K, Pattyn F, et al. Accurate normalization of real-time quantitative RT-PCR data by geometric averaging of multiple internal control genes. Genome Biol. 2002;3(7):Research0034.
2. Dysvik B, Jonassen I. J-Express: exploring gene expression data using Java. Bioinformatics. 2001;17(4):369-370.
3. Blom S, Paavolainen L, Bychkov D, et al. Systems pathology by multiplexed immunohistochemistry and whole-slide digital image analysis. Sci Rep. 2017;7(1):15580.
4. Leivonen SK, Pollari M, Bruck O, et al. T-cell inflamed tumor microenvironment predicts favorable prognosis in primary testicular lymphoma. Haematologica. 2019;104(2):338-346.
5. Challa-Malladi M, Lieu YK, Califano O, et al. Combined genetic inactivation of beta2-Microglobulin and CD58 reveals frequent escape from immune recognition in diffuse large B cell lymphoma. Cancer Cell. 2011;20(6):728-740.
6. Newman AM, Steen CB, Liu CL, et al. Determining cell type abundance and expression from bulk tissues with digital cytometry. Nat Biotechnol. 2019;37(7):773-782.
7. Reddy A, Zhang J, Davis NS, et al. Genetic and Functional Drivers of Diffuse Large B Cell Lymphoma. Cell. 2017;171(2):481-494.e415.
8. Schmitz R, Wright GW, Huang DW, et al. Genetics and Pathogenesis of Diffuse Large B-Cell Lymphoma. N Engl J Med. 2018;378(15):1396-1407.
9. Chapuy B, Stewart C, Dunford AJ, et al. Molecular subtypes of diffuse large B cell lymphoma are associated with distinct pathogenic mechanisms and outcomes. Nat Med. 2018;24(5):679-690.
10. Monti S, Savage KJ, Kutok JL, et al. Molecular profiling of diffuse large B-cell lymphoma identifies robust subtypes including one characterized by host inflammatory response. Blood. 2005;105(5):1851-1861.

Supplementary Tables

Supplementary Table S1. Patient characteristics for TME immune cell signature high and low groups

Characteristics	TME immune cell signature low n (%)	TME immune cell signature high n (%)	P-value[a]
Number of patients	61	20	
Gender			0.025
male	38 (62)	18 (90)	
female	23 (38)	2 (10)	
Age			0.179
<60	38 (62)	16 (80)	
≥60	23 (38)	4 (20)	
Stage			0.672
low	7 (11)	1 (5)	
high	54 (89)	19 (95)	
Molecular subtype[b]			0.069
GCB[c]	29 (48)	5 (25)	
non-GCB	16 (26)	10 (50)	
other	16 (26)	5 (25)	
WHO PS			1.000
0-1	36 (59)	12 (60)	
≥2	25 (41)	8 (40)	
IPI			0.376
0-2	16 (26)	3 (15)	
3-5	45 (74)	17 (85)	
LDH			0.103
low	9 (15)	0 (0)	
high	52 (85)	20 (100)	
EN			0.353
0-1	16 (26)	3 (15)	
≥2	32 (52)	14 (70)	
nd	13 (21)	3 (15)	

[a]Chi-square test (Fischer's Exact Test)

[b]Molecular subtype assesed using Hans algorithm

[c]GCB, germinal center B-cell like; nd, not determined; IPI, international prognostic index; LDH, lactate dehydrogenase

Supplementary Table S2. Median numbers of T-cells and their immunophenotypes in the TME

	Phenotype	Median (%)	Min (%)	Max (%)
From all cells				
T-cells	CD3+	16.24	0.06	69.07
	CD8+	6.14	0.19	29.86
	CD3+CD4+	5.45	0.03	42.36
	CD4+	14.11	0.50	59.15
Cytotoxic/active cells	GrB+	0.53	0.01	17.60
	Ki67+	14.61	0.27	33.93
	OX40+	0.11	0.01	4.53
	GrB+Ki67+	0.03	0.00	1.38
	GrB+OX40+	0.00	0.00	0.82
	Ki67+OX40+	0.01	0.00	0.50
	GrB+CD8+	0.07	0.00	3.21
	Ki67+CD8+	1.79	0.04	9.23
	OX40+CD8+	0.01	0.00	1.01
	GrB+Ki67+CD8+	0.01	0.00	1.23
	GrB+OX40+CD8+	0.00	0.00	0.24
	Ki67+OX40+CD8+	0.00	0.00	0.45
Immune checkpoint molecule positive cells	TIM3+	1.99	0.03	25.72
	LAG3+	0.27	0.01	5.56
	PD1+	1.05	0.00	24.44
	TIM3+LAG3+	0.10	0.00	1.94
	TIM3+PD1+	0.13	0.00	9.79
	LAG3+PD1+	0.07	0.00	1.34
	TIM3+CD4+CD3-	0.37	0.00	6.40
	LAG3+CD4+CD3-	0.01	0.00	0.88
Immune checkpoint molecule positive T-cells	TIM3+CD3+	1.02	0.00	15.01
	LAG3+CD3+	0.07	0.00	4.77
	LAG3+TIM3+CD3+	0.04	0.00	2.56
	TIM3+CD8+	0.21	0.00	7.31
	LAG3+CD8+	0.06	0.00	1.67
	PD1+CD8+	0.16	0.00	11.09
	TIM3+LAG3+CD8+	0.02	0.00	0.94
	TIM3+PD1+CD8+	0.02	0.00	2.28
	LAG3+PD1+CD8+	0.01	0.00	0.26
	TIM3+CD3+CD4+	0.52	0.00	12.48
	LAG3+CD3+CD4+	0.03	0.00	2.10
	TIM3+LAG3+CD3+CD4+	0.02	0.00	1.12
	TIM3+CD3+CD4-	0.38	0.00	6.79
	LAG3+CD3+CD4-	0.03	0.00	2.76
Regulatory T-cells	FOXP3+	2.25	0.10	29.21
	FOXP3+CD3+CD4+	0.44	0.00	7.80
Th1-cells	TBET+	0.09	0.02	1.13
	TBET+CD3+CD4+	0.00	0.00	0.32
Cell immunophenotype ratios				
Cytotoxic cells	GrB+CD8+/CD8+	1.04	0.00	18.94
	Ki67+CD8+/CD8+	25.44	0.80	88.09
	OX40+CD8+/CD8+	0.20	0.00	31.73
	GrB+Ki67+CD8+/CD8+	0.15	0.00	11.51
Immune checkpoint molecule positive cells	TIM3+CD3+/CD3+	7.21	0.00	37.42
	LAG3+CD3+/CD3+	0.59	0.00	12.52
	TIM3+LAG3+CD3+/CD3+	0.29	0.00	6.39
	TIM3+CD8+/CD8+	5.57	0.13	68.80
	LAG3+CD8+/CD8+	1.45	0.00	20.95
	PD1+CD8+/CD8+	3.78	0.01	56.87
	TIM3+LAG3+CD8+/CD8+	0.52	0.00	19.66
	TIM3+PD1+CD8+/CD8+	0.47	0.00	38.82
	LAG3+PD1+CD8+/CD8+	0.25	0.00	20.06
	TIM3+CD3+CD4+/CD3+CD4+	8.50	0.00	43.26
	LAG3+CD3+CD4+/CD3+CD4+	0.51	0.00	10.29
	LAG3+TIM3+CD3+CD4+/CD3+CD4+	0.27	0.00	5.47
	TIM3+CD4+CD3-/CD4+CD3-	3.46	0.00	29.52
Regulatory T-cells	FOXP3+CD3+CD4+/CD3+CD4+	14.61	0.15	51.39
Th1-cells	TBET+CD3+CD4+/CD3+CD4+	0.04	0.00	7.01

Supplementary Table S3. Association of B2M and HLA expression with the molecular subtypes

A

	GCB n (%)	non-GCB n (%)	nd n (%)	P-value[a]
B2M expression				0.007
Negative	19 (25)	9 (12)	1 (8)	
Misplaced	3 (4)	9 (12)	0 (0)	
Moderate	48 (62)	31 (42)	8 (62)	
Positive	7 (9)	25 (34)	4 (31)	

[a]Kruskal-Wallis H test

B

	GCB n (%)	non-GCB n (%)	nd n (%)	P-value[a]
HLA-ABC expression				0.219
Negative	2 (3)	4 (5)	0 (0)	
Moderate	45 (60)	31 (41)	7 (50)	
Positive	28 (37)	40 (53)	7 (50)	

[a]Kruskal-Wallis H test

C

	GCB n (%)	non-GCB n (%)	nd n (%)	P-value[a]
HLA-DR expression				0.201
Negative	12 (15)	19 (25)	2 (14)	
Moderate	36 (46)	34 (45)	10 (71)	
Positive	30 (38)	22 (29)	2 (14)	

[a]Kruskal-Wallis H test

Supplementary Table S4. Association of the expression of immune checkpoint molecules in the TME with HLA-ABC expression in the HEL-DLBCL cohort

A

	low TIM3, LAG3, PD1 n (%)	high TIM3, LAG3, PD1 n (%)	P-value[a]
HLA-ABC expression			0.037
Negative	3 (4)	0 (0)	
Moderate	37 (54)	20 (40)	
Positive	29 (42)	30 (60)	

[a]Kruskal-Wallis H test

B

	low TIM3, LAG3, PD1 n (%)	high LAG3+ n (%)	only high TIM3+ n (%)	P-value[a]
HLA-ABC expression				0.067
Negative	3 (4)	0 (0)	0 (0)	
Moderate	37 (54)	11 (34)	9 (50)	
Positive	29 (42)	21 (66)	9 (50)	

[a]Kruskal-Wallis H test

Supplementary Table S5. Expression of selected immune checkpoint genes imputed by CIBERSORTx.

A. Nanostring cohort (n=81)

Gene Symbol	CD8 T-cells	CD4 T-cells	NK cells	Monocytes/ Macrophages	Dendritic cells	Neutrophils
HAVCR2 (TIM3)	10.06	10.11	9.43*	7.93	0	0
LAG3	11.52	10.13	8.94*	6.74*	0	0
PDCD1 (PD1)	7.94	8.65	0	0	10.62*	0

*inadequate statistical power

B. Monti et al. (n=176)

Gene Symbol	CD8 T-cells	CD4 T-cells	NK cells	Monocytes/ Macrophages	Dendritic cells	Neutrophils
HAVCR2 (TIM3)	11.54	8.38*	0	10.62	0	0
LAG3	10.83	10.5	0	0	0	0
PDCD1 (PD1)	8.54	9.41	9.61	0	10.49*	0

*inadequate statistical power

C. Reddy et al. (n=624)

Gene Symbol	CD8 T-cells	CD4 T-cells	NK cells	Monocytes/ Macrophages	Dendritic cells	Neutrophils
HAVCR2 (TIM3)	5.91	0	5.93	5.49	0	7.62
LAG3	7.24	5.08	7.25	0	0	0
PDCD1 (PD1)	4.49	5.25	0	0	0	0

* inadequate statistical power

D. Schmitz et al. (n=562)

Gene Symbol	CD8 T-cells	CD4 T-cells	NK cells	Monocytes/ Macrophages	Dendritic cells	Neutrophils
HAVCR2 (TIM3)	13.36	0	0	11.35	0	15.17
LAG3	13.78	12.03*	14.52	0	0	0
PDCD1 (PD1)	11.61	12.34	0*	0*	0	0

* inadequate statistical power

E. Chapuy et al. (n=137)

Gene Symbol	CD8 T-cells	CD4 T-cells	NK cells	Monocytes/ Macrophages	Dendritic cells	Neutrophils
HAVCR2 (TIM3)	10.34	8.54*	0	9.79	0	12.05
LAG3	7.09*	7.74*	10.94*	0	0	9.82*
PDCD1 (PD1)	5.71*	6.73	8.42	4.36*	7.25	0

* inadequate statistical power

Supplementary Table S6. Correlation between TIM3 expression in the NLG Trial cohort and gene expression of cytokines in the Nanostring nCounter Human PanCancer Immuneprofiling Panel (n=42)

	Spearman's Rho	P-value
IL22RA2	-0.465	0.0019
GZMB	0.458	0.0023
IFNG	0.449	0.0029
IL17RA	0.431	0.0043
IL6R	0.415	0.0063
IL15RA	0.413	0.0065
IL10	0.400	0.0087
IL2RB	0.361	0.019
IL1B	0.349	0.023
IL11	-0.344	0.026
IL10RA	0.337	0.029
IL1A	-0.314	0.043
IL32	0.312	0.044
IL1RN	0.305	0.050
CD44	0.290	0.062
IL22RA1	-0.290	0.062
IL1RL1	-0.282	0.070
IL34	-0.280	0.072
IL13	-0.265	0.090
IL2RG	0.262	0.094
IL18RAP	0.257	0.100
IL1R1	-0.252	0.108
IL12B	-0.250	0.111
IL2RA	0.226	0.150
IL1RAPL2	-0.221	0.160
IFNL1	-0.204	0.195
IL4	-0.187	0.235
IL16	0.173	0.275
IL8	0.149	0.346
IL18R1	-0.149	0.346
IL23A	-0.144	0.363
IL6	0.139	0.378
IL26	-0.136	0.390
IL7	-0.134	0.397
IL1RAP	-0.130	0.412
ILF3	-0.127	0.423
IL17RB	0.108	0.497
IL12RB2	-0.097	0.541
IL24	0.091	0.566
IL1R2	0.089	0.574
IL7R	-0.089	0.575
IL12A	0.089	0.576
IL11RA	-0.082	0.604
IL15	0.077	0.629
TNFRSF4	0.075	0.636
IL3RA	0.068	0.669
IL21R	0.064	0.688
ICOS	-0.050	0.752
IL13RA1	-0.047	0.767
IL12RB1	-0.046	0.774
IL4R	-0.041	0.799
IL6ST	0.031	0.845
IL21	0.020	0.901
IL18	0.010	0.948

Supplementary Table S7. Patient characteristics for cytotoxicity low and high groups

Characteristics	Cytotoxicity low n (%)	Cytotoxicity high n (%)	P-value[a]
Number of patients	102	17	
Gender			0.796
male	58 (57)	9 (53)	
female	44 (43)	8 (47)	
Age			0.032
<60	49 (48)	3 (18)	
≥60	53 (52)	14 (82)	
Stage			0.184
low	62 (61)	7 (41)	
high	40 (39)	10 (59)	
Molecular subtype[b]			0.104
GCB[c]	45 (44)	4 (24)	
non-GCB	47 (46)	12 (71)	
other	10 (10)	1 (6)	
IPI			0.051
0-2	72 (71)	8 (47)	
3-5	28 (27)	9 (53)	
nd	2 (2)	0 (0)	
LDH			0.792
low	49 (48)	7 (41)	
high	52 (51)	9 (53)	
nd	1 (1)	1 (6)	
Treatment			0.800[d]
R-CHOP	91 (89)	15 (88)	
R-CHOEP	8 (8)	1 (6)	
other	3 (3)	1 (6)	

[a]Chi-square test (Fischer's Exact Test)

[b]Molecular subtype assesed using Hans algorithm

[c]GCB, germinal center B-cell like; nd, not determined; IPI, international prognostic index; LDH, lactate dehydrogenase; R-CHOP, rituximab, cyclophosphamide, doxorubicine, vincristine, prednisone; R-CHOEP, R-CHOP+etoposide

[d]Kruskal-Wallis H test

Supplementary Table S8. Patient characteristics for Treg low and high groups

Characteristics	Treg low n (%)	Treg high n (%)	P-value[a]
Number of patients	32	14	
Gender			0.742
male	21 (66)	8 (57)	
female	11 (34)	6 (43)	
Age			0.497
<60	21 (66)	11 (79)	
≥60	11 (34)	3 (21)	
Stage			0.574
low	2 (6)	2 (14)	
high	30 (94)	12 (86)	
Molecular subtype[b]			0.468
GCB[c]	14 (44)	7 (50)	
non-GCB	12 (38)	3 (21)	
other	2 (6)	3 (21)	
nd	4 (13)	1 (7)	
IPI			0.684
low	5 (66)	3 (64)	
high	27 (34)	11 (36)	
LDH			0.633
low	3 (9)	2 (14)	
high	29 (91)	12 (86)	

[a]Chi-square test (Fischer's Exact Test)

[b] Molecular subtype assesed using Hans algorithm

[c]GCB, germinal center B-cell like; nd, not determined; IPI, international prognostic index; LDH, lactate dehydrogenase; R-CHOP, rituximab, cyclophosphamide, doxorubicine, vincristine, prednisone; R-CHOEP, R-CHOP+etoposide

Supplementary Figure Legends

Supplementary Figure S1: TME associated signatures revealed by gene expression analysis. A) Correlation between the B-cell signature and the TME immune cell signature. The y-axis depicts the median expression of all genes included in the B-cell signature, and the x-axis depicts the median expression of all genes included in the TME immune cell signature. B-E) Unsupervised hierarchical clustering of gene signatures identified by correlation matrix analyses. Genes are depicted in the rows and patients are depicted in the columns. F) Kaplan-Meier (log-rank test) survival plots depict OS and PFS in the TME immune cell signature high and low groups.

Supplementary Figure S2: Correlation between gene and protein expression. A-J) Correlation (Spearman rank) between the expression of distinct T-cell markers with the corresponding gene expression. The amount of cells staining positive for a certain marker is depicted on the y-axis and corresponding gene expression is depicted on the x-axis.

Supplementary Figure S3: Multiplex immunohistochemistry reveals significant heterogeneity in the DLBCL TME. Heatmap visualizing all quantified immune cells and their immunophenotypes organized by unsupervised hierarchical clustering

Supplementary Figure S4: PFS between patients with high and low expression of immune checkpoint molecules in the TME. A-B) Kaplan-Meier (log-rank test) survival plots depict progression-free survival (PFS) in the groups with high and low amount of immune checkpoint molecule expressing T-cells in the NLG Trial (n=46) (A) and the HEL-DLBCL (n=119) (B) cohorts.

Supplementary Figure S5: Impact of immune checkpoint molecule expressing T-cells on survival in patients with an IPI score over 1 and according to molecular subtype in the HEL-

DLBCL cohort. A) Kaplan-Meier (log-rank test) survival plots depict PFS in the groups with high and low amount of immune checkpoint molecule expressing T-cells in patients with an IPI score over 1 in the HEL-DLBCL cohort. B) Kaplan-Meier (log-rank test) survival plots depict PFS in the groups with high and low amount of immune checkpoint molecule expressing T-cells in patients with non-GCB DLBCL. C-D) Kaplan-Meier (log-rank test) survival plots depict overall survival (OS) (C) and PFS (D) in the groups with high and low amount of immune checkpoint molecule expressing T-cells in patients with GCB DLBCL.

Supplementary Figure S6: The impact of immune checkpoint molecules and distinct T-cell subtypes on PFS. A-B) Forest plots visualizing the impact of the proportion of T-cells ($CD3^+$-cells) and selected T-cell subtypes, expression of immune checkpoint molecules and ratios of $TIM3^+$-cells on PFS in the NLG Trial (A) and HEL-DLBCL (B) cohorts using continuous variables, as evaluated using Cox univariate test.

Supplementary Figure S7: Multivariate analyses of TIM3 and TIM3 expressing T-cells with IPI and COO. A-D) Forest plots visualizing the impact of TIM3 and TIM3 expressing T-cell subtypes on OS in the NLG Trial (A) and HEL-DLBCL cohorts (B) and PFS in the NLG Trial (C) and HEL-DLBCL cohorts (D) using continuous variables, as evaluated using Cox multivariate test with IPI as a continuous variable and COO with GCB subtype as reference.

Supplementary Figure S8: Characterization of cytotoxic cells in the TME. A) Unsupervised hierarchical clustering of cytotoxicity related markers in the HEL-DLBCL cohort. B) Kaplan-Meier (log-rank test) survival plots depict OS and PFS in the Granzyme high and low groups of the HEL-DLBCL cohort. C) Kaplan-Meier (log-rank test) survival plots depict OS and PFS in the OX40 high and low groups of the HEL-DLBCL cohort.

Supplementary Figure S9: Characterization of Tregs in the TME. A) Unsupervised hierarchical clustering of $FOXP3^+$ cells in the NLG Trial cohort. B) Kaplan-Meier (log-rank test) survival plots depict OS and PFS in the groups with a larger and smaller proportion of Tregs in the TME in the NLG Trial cohort.

Supplementary Figures

Supplementary Figure S1. TME associated signatures revealed by gene expression analysis

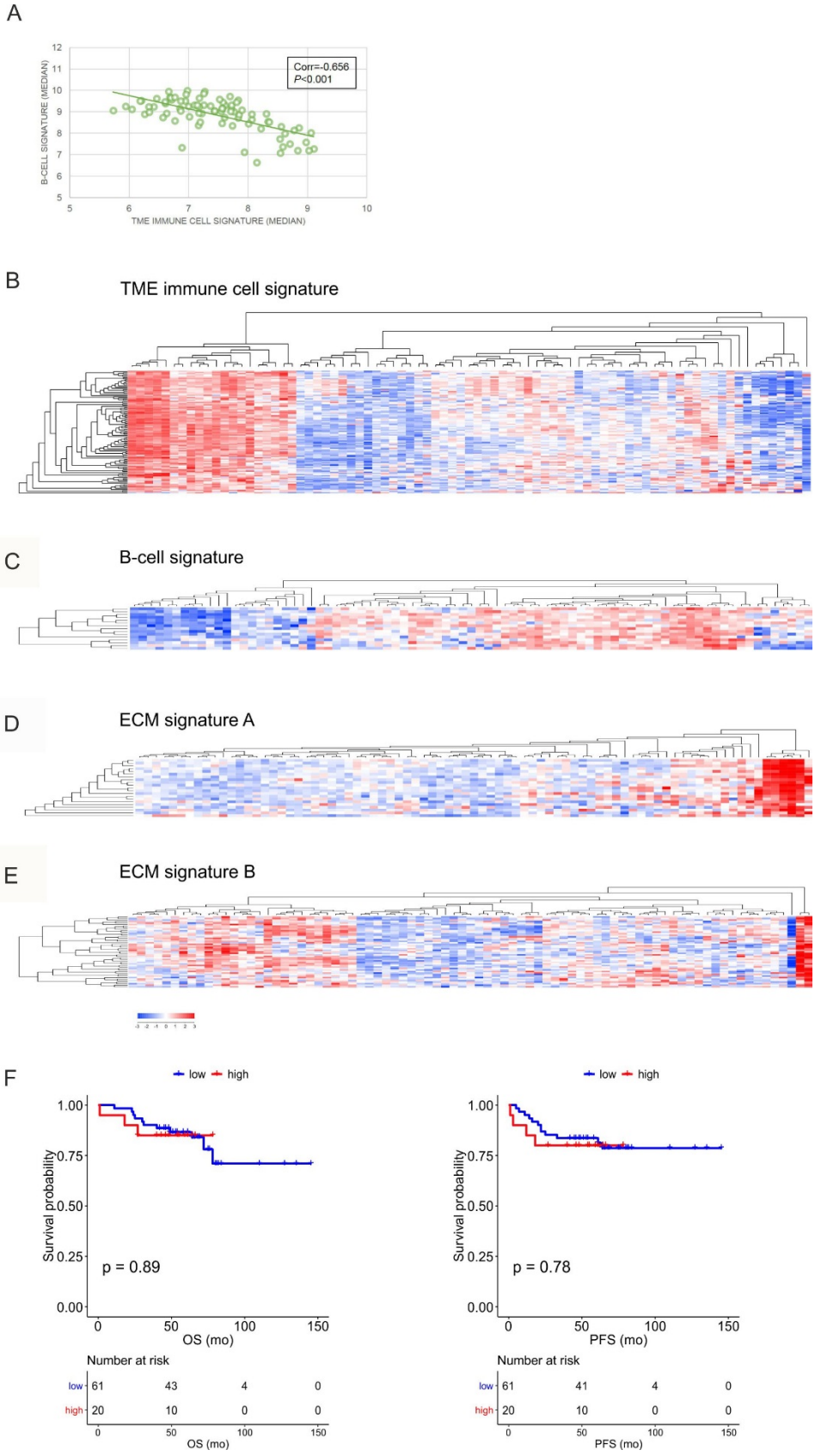

Supplementary Figure S2. Correlation between gene and protein expression

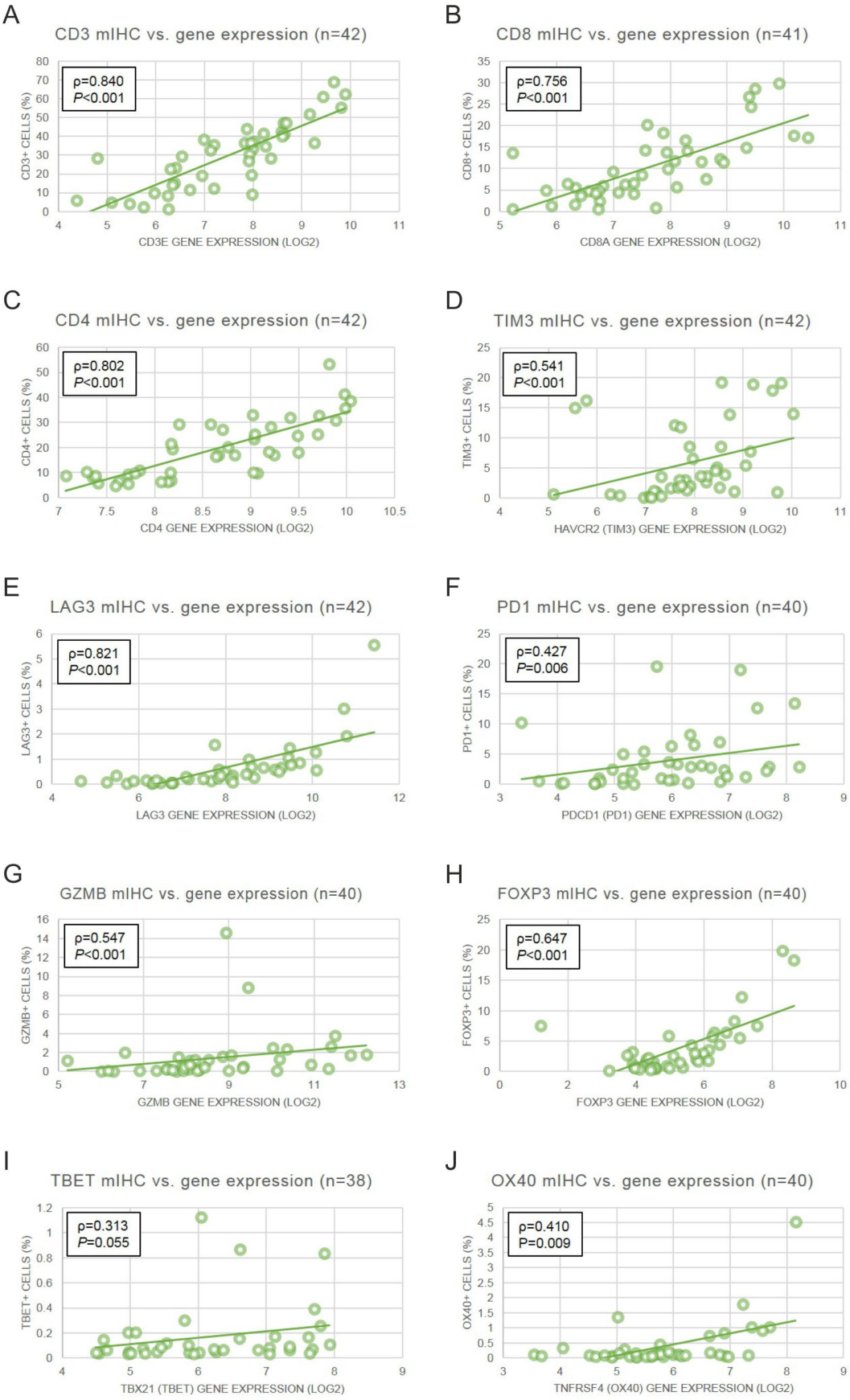

Supplementary Figure S3: Multiplex immunohistochemistry reveals significant heterogeneity in the DLBCL TME

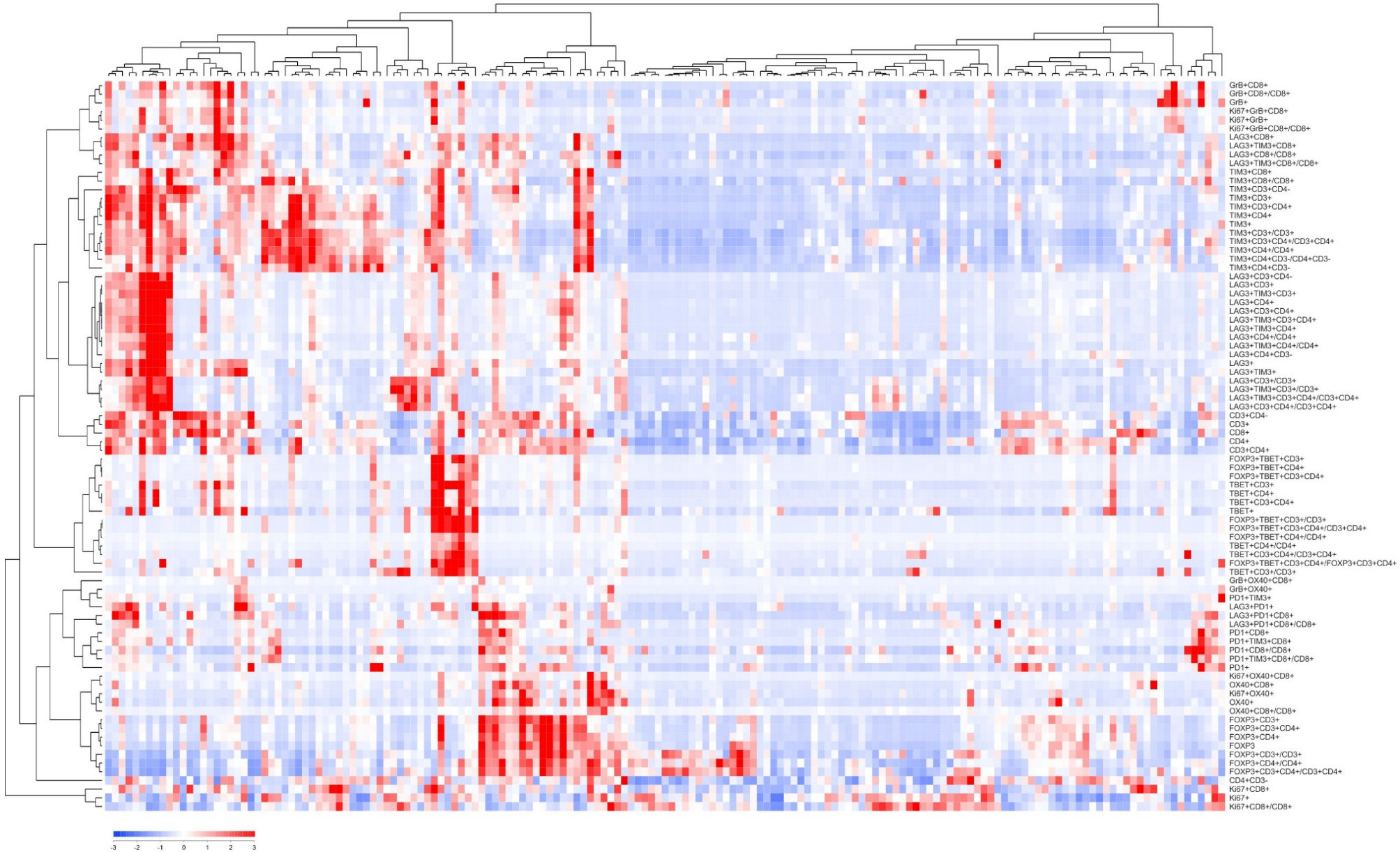

Supplementary Figure S4. PFS between patients with or without high expression of immune checkpoint molecules in the TME

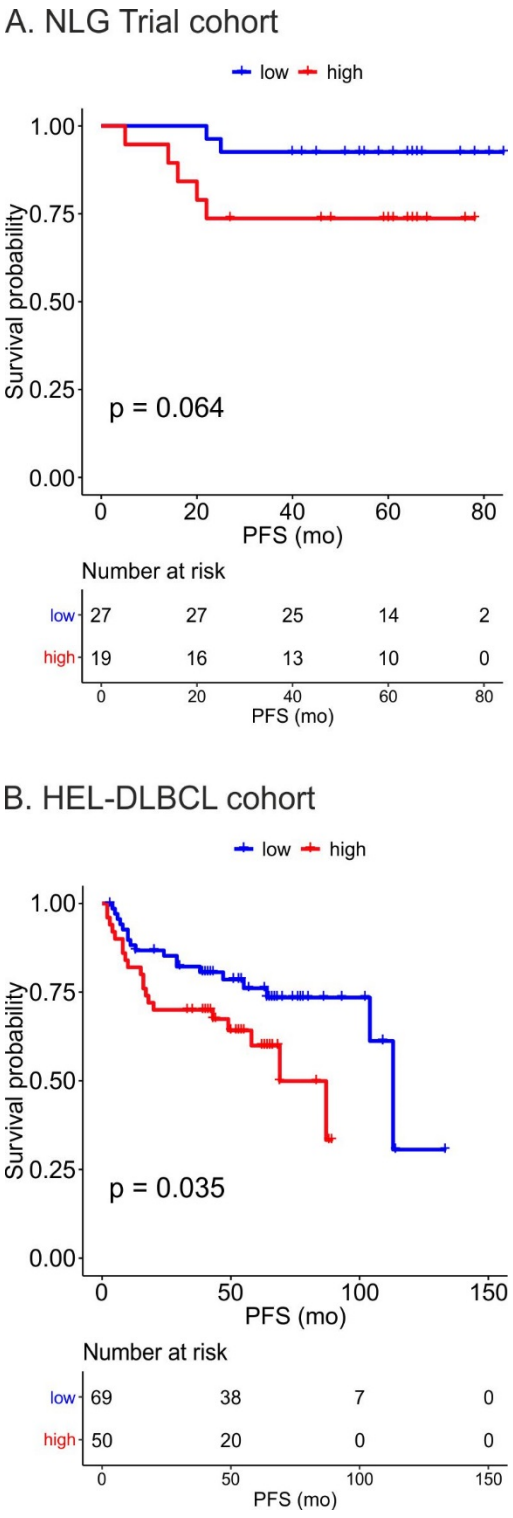

Supplementary Figure S5. Impact of T-cells expressing immune checkpoint molecules on survival in patients with an IPI score over 1 and according to molecular subtype in the HEL-DLBCL cohort

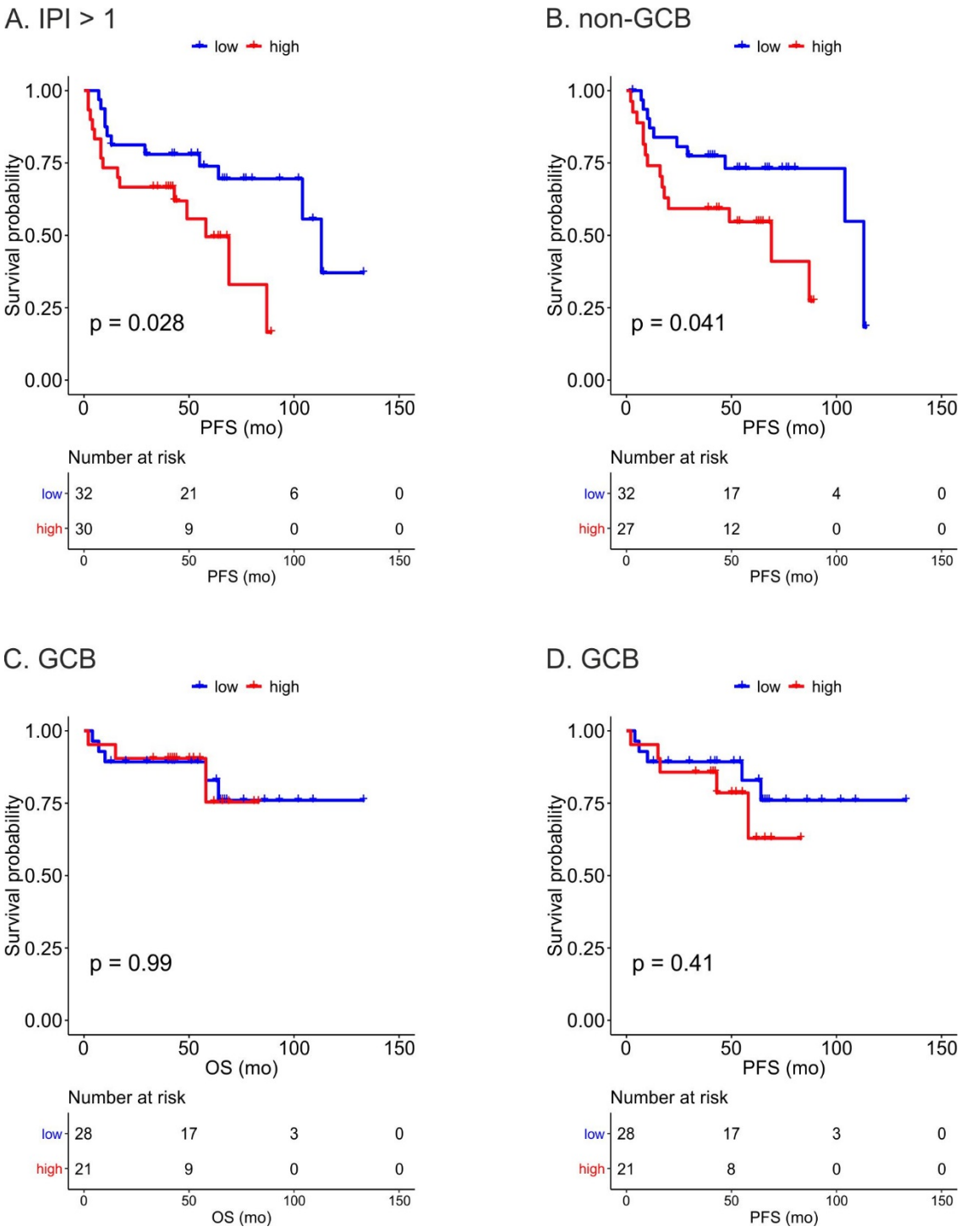

Supplementary Figure S6. The impact of immune checkpoint molecules and distinct T-cell subtypes on PFS

A. NLG-Trial cohort

Cell type	HR (95% CI)	P-value
CD3+ (n=51)	1.09 (0.73-1.60)	0.668
CD4+ (n=51)	1.30 (0.73-2.30)	0.377
CD3+CD4+ (n=51)	1.31 (0.69-2.50)	0.409
CD8+ (n=50)	0.66 (0.21-2.10)	0.486
Immune checkpoint molecules		
LAG3+ (n=51)	0.89 (0.00-3500)	0.977
PD1+ (n=49)	1.44 (0.37-5.60)	0.594
TIM3+ (n=51)	2.45 (0.94-6.40)	0.067
TIM3+ cells (ratios)		
TIM3+CD3+/CD3+ (n=51)	1.70 (0.86-3.40)	0.127
TIM3+CD4+/CD4+ (n=51)	1.62 (0.83-3.20)	0.158
TIM3+CD3+CD4+/CD3+CD4+ (n=51)	1.40 (0.77-2.60)	0.266
TIM3+CD8+/CD8+ (n=49)	0.83 (0.00-170)	0.946
TIM3+CD4+CD3-/CD4+CD3- (n=51)	2.10 (0.92-4.80)	0.079

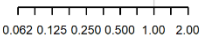

B. HEL-DLBCL cohort

Cell type	HR (95% CI)	P-value
CD3+ (n=137)	1.04 (0.83-1.30)	0.716
CD4+ (n=137)	1.02 (0.79-1.30)	0.865
CD3+CD4+ (n=137)	1.10 (0.76-1.60)	0.602
CD8+ (n=130)	0.79 (0.47-1.30)	0.372
Immune checkpoint molecules		
LAG3+ (n=137)	1.21 (0.02-82.0)	0.928
PD1+ (n=128)	1.82 (0.62-5.30)	0.274
TIM3+ (n=137)	2.17 (1.20-3.90)	0.010
TIM3+ cells (ratios)		
TIM3+CD3+/CD3+ (n=136)	1.46 (1.00-2.00)	0.026
TIM3+CD4+/CD4+ (n=136)	1.56 (1.10-2.20)	0.013
TIM3+CD3+CD4+/CD3+CD4+ (n=136)	1.35 (1.00-1.80)	0.034
TIM3+CD8+/CD8+ (n=128)	0.52 (0.02-13.0)	0.692
TIM3+CD4+CD3-/CD4+CD3- (n=136)	1.95 (1.30-3.00)	0.002

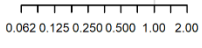

Supplementary Figure S7. Multivariate analyses of TIM3 and TIM3 expressing T-cells with IPI and COO

A. NLG Trial cohort

OS	HR (95% CI)	P-value
TIM3+	5.14 (1.30-20.41)	0.020
IPI	0.82 (0.26-2.58)	0.729
Subtype	1.89 (0.22-16.64)	0.565
TIM3+CD4+CD3-/CD4+CD3-	3.09 (1.01-9.45)	0.048
IPI	0.97 (0.30-3.09)	0.953
Subtype	2.22 (0.28-17.36)	0.448

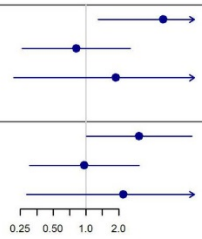

B. HEL-DLBCL cohort

OS	HR (CI 95%)	P-value
TIM3+	2.6 (1.3-5.0)	0.007
IPI	1.8 (1.3-2.4)	<0.001
Subtype	1.8 (0.8-4.0)	0.158
TIM3+CD3+/CD3+	1.5 (0.96-2.3)	0.076
IPI	1.7 (1.29-2.3)	<0.001
Subtype	1.7 (0.76-3.9)	0.196
TIM3+CD4+/CD4+	1.7 (1.13-2.6)	0.011
IPI	1.7 (1.29-2.3)	<0.001
Subtype	1.9 (0.82-4.2)	0.137
TIM3+CD3+CD4+/CD3+CD4+	1.4 (1.01-2.0)	0.046
IPI	1.6 (1.23-2.1)	<0.001
Subtype	1.4 (0.66-3.0)	0.37
TIM3+CD4+CD3-/CD4+CD3-	2.0 (1.23-3.2)	0.005
IPI	1.7 (1.26-2.3)	<0.001
Subtype	1.7 (0.78-3.9)	0.178

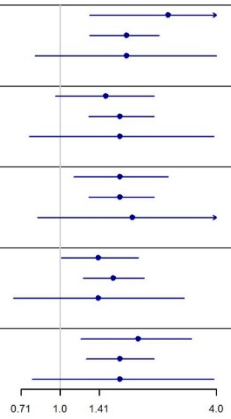

C. NLG Trial cohort

PFS	HR (95% CI)	P-value
TIM3+	2.83 (0.86-9.27)	0.085
IPI	1.48 (0.55-4.00)	0.442
Subtype	0.88 (0.14-5.52)	0.889
TIM3+CD4+CD3-/CD4+CD3-	2.03 (0.74-5.54)	0.169
IPI	1.62 (0.59-4.50)	0.351
Subtype	1.12 (0.18-6.99)	0.900

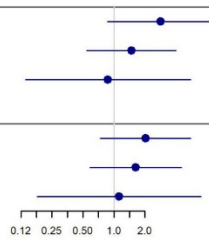

D. HEL-DLBCL cohort

PFS	HR (CI 95%)	P-value
TIM3+	2.2 (1.14-4.2)	0.019
IPI	1.7 (1.29-2.2)	<0.001
Subtype	1.7 (0.82-3.6)	0.155
TIM3+CD3+/CD3+	1.4 (0.98-2.1)	0.065
IPI	1.7 (1.27-2.2)	<0.001
Subtype	1.6 (0.77-3.4)	0.206
TIM3+CD4+/CD4+	1.6 (1.06-2.4)	0.025
IPI	1.7 (1.26-2.2)	<0.001
Subtype	1.7 (0.83-3.6)	0.146
TIM3+CD3+CD4+/CD3+CD4+	1.4 (0.97-1.9)	0.072
IPI	1.7 (1.27-2.2)	<0.001
Subtype	1.6 (0.78-3.5)	0.189
TIM3+CD4+CD3-/CD4+CD3-	1.8 (1.14-2.9)	0.012
IPI	1.6 (1.24-2.1)	<0.001
Subtype	1.6 (0.79-3.5)	0.186

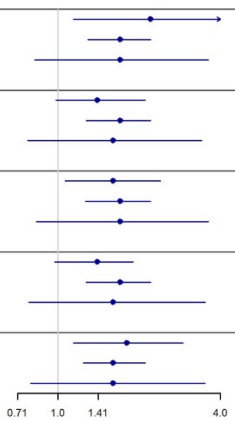

Supplementary Figure S8. Characterization of cytotoxic cells in the TME

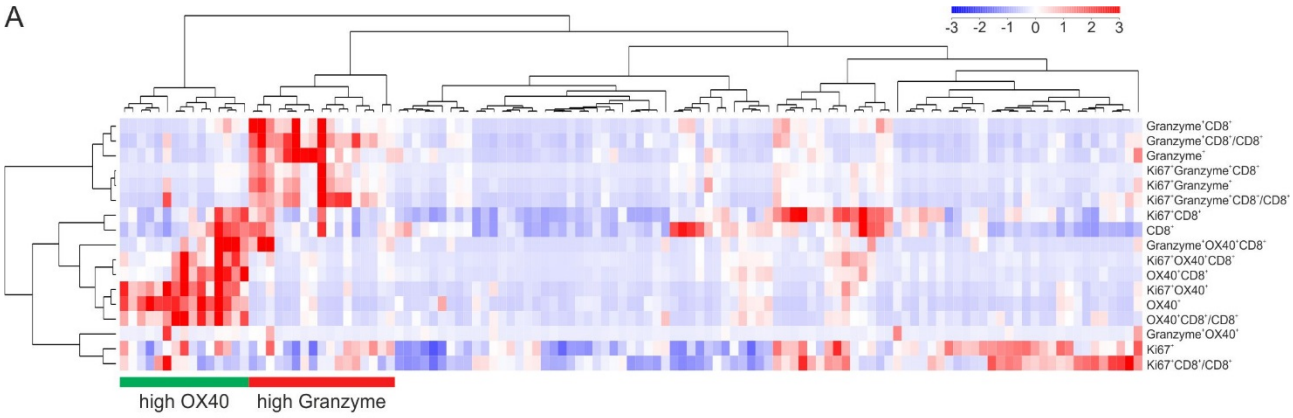

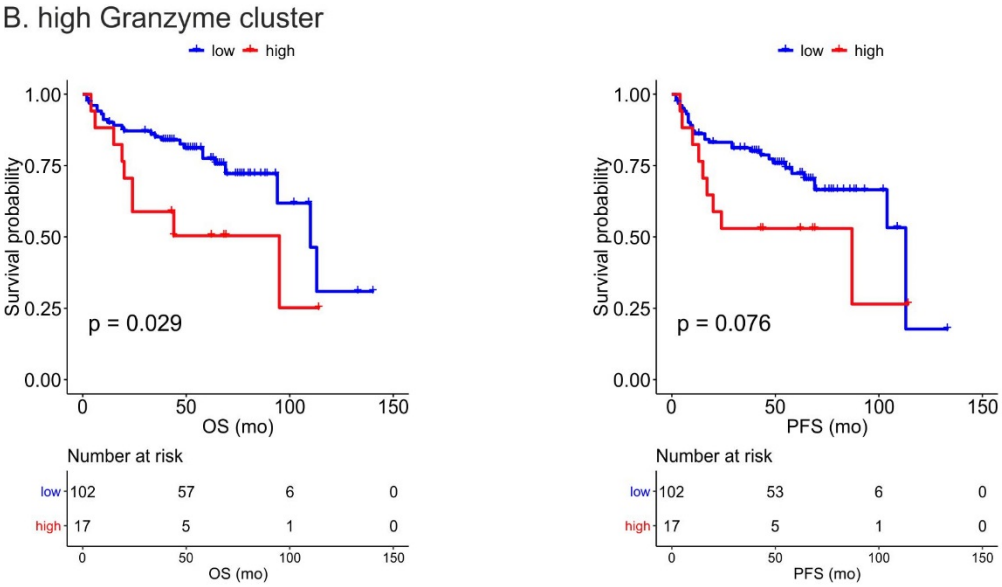

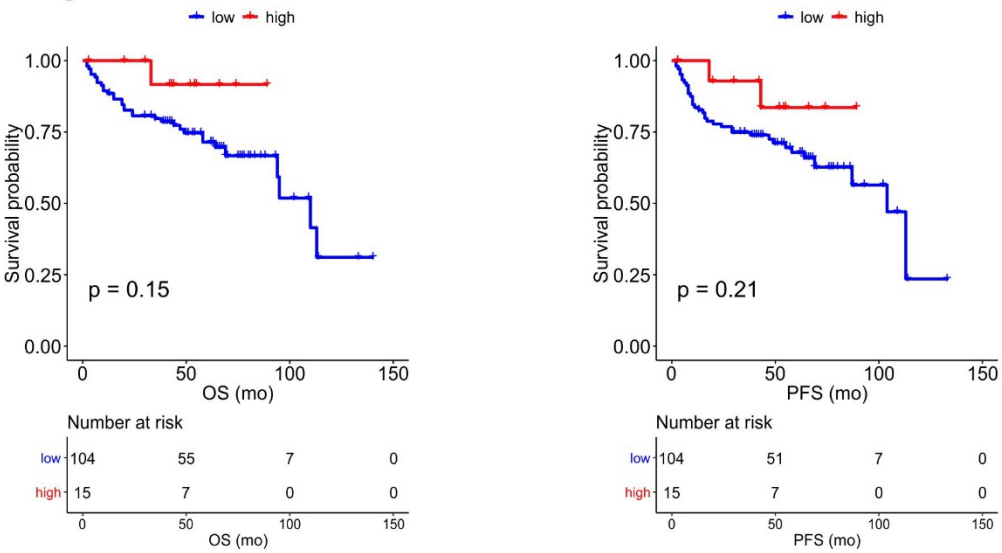

Supplementary Figure S9. Characterization of Tregs in the TME